Optimum Pole Number Combination for High-Speed High-Power BPM Bearingless Motor

Zongwei Liu, Akira Chiba

Tokyo Institute of Technology, Ookayama 2-12-1, Meguro-ku, 152-8550 Tokyo, Japan, liu.z.ad@m.titech.ac.jp

***Abstract*—Pole number combination of torque and suspension winding is essential for bearingless motors. In this paper, the comparison of the performance of a high-speed high-power buried permanent magnet bearingless motor with different pole combinations is presented. The power factor, efficiency, suspension force amplitude, fluctuation and eddy current are compared for a 35 kW unit.**

I. INTRODUCTION

In a bearingless motor, electromagnetic force is used to suspend the rotor, thus, mechanical bearings are not needed. The rotor rotates without mechanical a contact, therefore, no lubricating oil is required and friction is small. Besides, compactness, high speed, long-life, and easy maintenance are also the advantages of a bearingless motor. Applications of bearingless motor include liquid pumps, artificial hearts and so on.

Applications such as compressors require high speed and high power motors [1-2]. In [3], a bearingless motor of 30000 r/min and 114 kW is designed. And in [4], a bearingless motor of 30000 r/min and 5 kW is proposed. For a high speed bearingless motor, a proper pole combination of torque and suspension can improve the performance. Simulation for different pole pair combinations of a concentrated winding SPM bearingless motor was conducted in [5]. Harmonics, eddy current and suspension force ripple of different pole pair combinations for the SPM bearingless motor were studied in [6]. However, the torque performance is not taken into consideration. The vibration with different pole pair combinations for SPM bearingless motor is compared in [7].

In this paper, the number of pole combination of torque and suspension of a BPM bearingless motor at a speed of 45000 r/min and an output of 35 kW is investigated. The torque performance, suspension performance and rotor eddy current are compared. It is found that increasing pole number of torque winding will reduce the power factor. Moreover, better suspension performance and lower eddy current loss can be achieved when the pole number of suspension winding is 2 more with respect to the pole number of torque winding. FEM 2D analysis is conducted.

II. WORKING PRINCIPLE OF BPM BEARINGLESS MOTOR

Fig. 1 shows the cross section of the prototype motor. The stator has 36 slots and two sets of three-phase windings for the torque generation and suspension force generation. There are 24 permanent magnets buried in the rotor. The rotor pole number can be adjusted by changing PM magnetization directions.

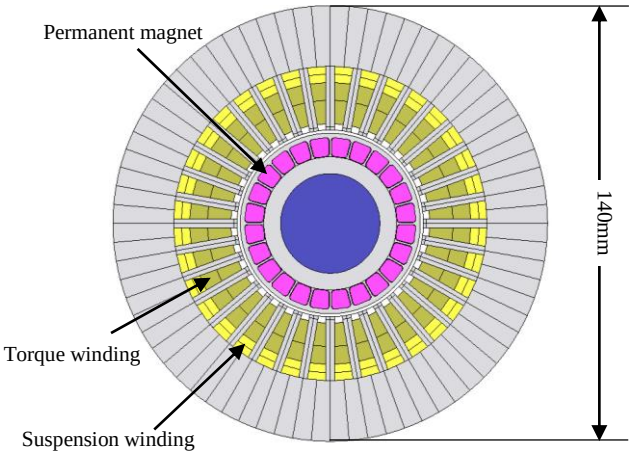

Figure 1. Prototype motor.

TABLE I. COMBINATIONS OF POLES.

P_1	2	4	4	6	6	8
P_2	4	2	6	4	8	6

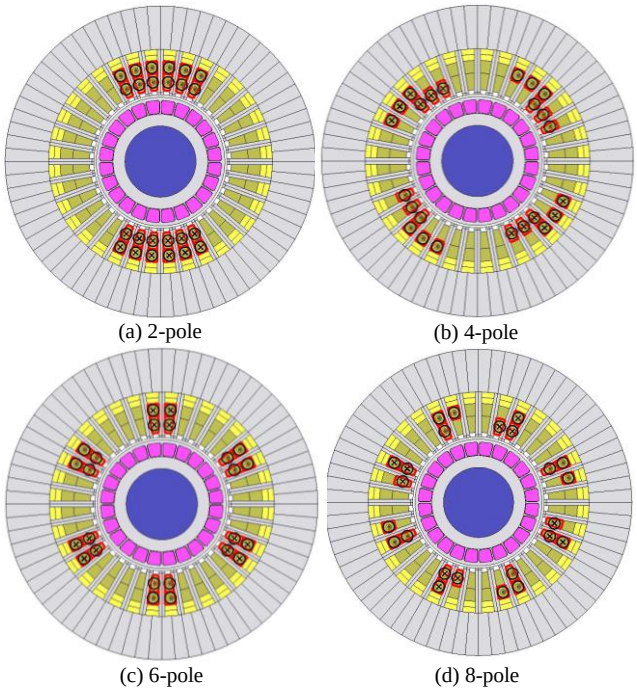

Figure 2. Torque windings.

Let us define P_1 as the pole number of torque generation and P_2 as the pole number of suspension force generation, P_1 and P_2 should satisfy the equation $P_2 = P_1 \pm 2$. Possible pole number combinations are shown in Table I. The six combinations will be analyzed from 2-pole to 8-pole. In Fig. 2 and Fig. 3, the torque and suspension windings are shown respectively.

In Fig. 4, a principle of suspension force generation of the 4-2 combination is shown. There are four-pole permanent magnets in the rotor. There are four pole windings for torque generation and also two-pole windings for suspension force generation. When there is current flowing in the 2-pole windings, magnetic fluxes are generated as shown by the broken lines. The magnetic fluxes generated by current and permanent magnets are in the same direction in airgap 1 while it is opposite direction in airgap 3. So the flux density will be increased in airgap 1 and decreased in airgap 3. Hence, a suspension force in the positive direction of x-axis is generated. By choosing proper current phase angle, suspension force in any direction can be generated. The suspension forces are generated by force commands in negative feedback loops of the magnetic suspension.

III. TORQUE PERFORMANCE COMPARISION

A. Torque Current Calculation

When the motor rotates at rated speed of 45000 r/min, the fundamental amplitude U_{emf} of the back e.m.f generated in torque windings is shown in Table II. When the number of poles is increased, the back e.m.f is decreased. The airgap power P is calculated as [4]

$$P = 3 \cdot \frac{U_{emf}}{\sqrt{2}} \cdot \frac{I_q}{\sqrt{2}}. \tag{1}$$

P is assumed to be 35 kW, thus the required amplitudes of the torque current I_q are calculated and shown in Table II. It is observed that U_{emf} decreases as the pole number increases, which leads to an increased torque current.

The rotation speed is 45000 r/min, so the rotation at angular shaft speed ω_r and torque current angular frequency ω_c can be calculated as

$$\omega_r = 2 \cdot \pi \cdot \frac{45000}{60} = 1500\pi. \tag{2}$$

$$\omega_c = 2 \cdot \pi \cdot \frac{45000}{60} \cdot \frac{P_1}{2} = 750 \cdot \pi \cdot P_1. \tag{3}$$

Thus, the rated torque is calculated as

$$T = \frac{P}{\omega_r} = 7.4Nm. \tag{4}$$

In Fig. 5, the analysis results of the torque when the current is increased in intervals of 70A are shown. It indicates that as the pole number increases, an increased current is needed to generate the rated torque.

B. Power Factor Comparision

The terminal voltage U_p is expressed as

$$U_p = R \cdot I_q + j\omega_c \cdot L \cdot I_q + U_{emf}. \tag{5}$$

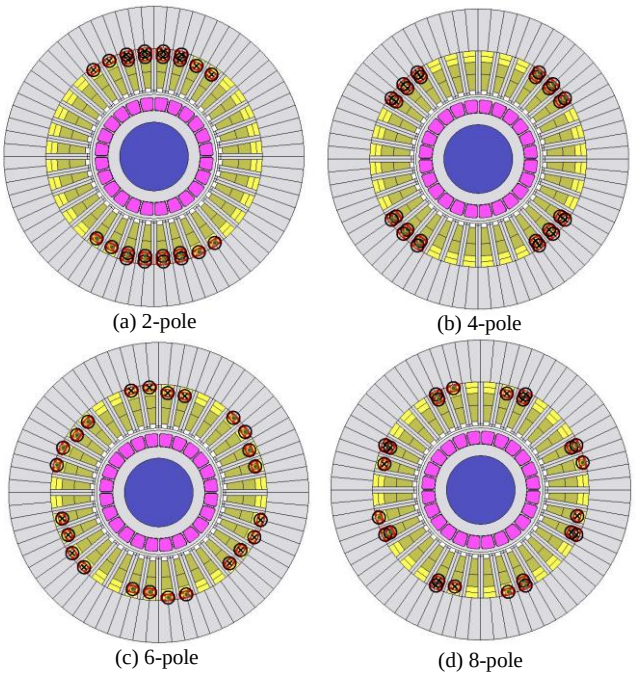

Figure 3. Suspension windings.

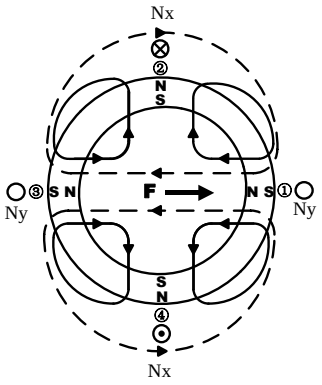

Figure 4. Principle of suspension force.

TABLE II. BACK E.M.F AND TORQUE CURRENT.

P_1	U_{emf} [V]	I_q [A]
2	114	203
4	100	230
6	94	245
8	84	276

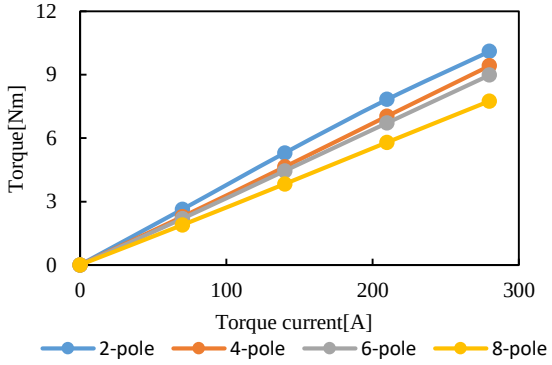

Figure 5. Principle of suspension force.

where, R is the phase resistance and L is the phase inductance. The phasor diagram is shown in Fig. 6. The fundamental power factor is cosφ, in which φ is the phase difference between phase voltage and phase current. From Fig. 6, L can be written as

$$L = \frac{U_p \sin\varphi}{\omega_c \cdot I_q}. \quad (6)$$

The power factor and the phase inductance are shown in Table III. It is found that the power factor is decreasing with the increase of pole number of torque generation. P1=6 and P1=8 are not good choices since power factors are less than 0.85. The voltage drop of R is negligible, thus φ can be calculated as

$$\varphi \approx \arctan\left(\frac{\omega_c \cdot L \cdot I_q}{U_{emf}}\right). \quad (7)$$

Combining (3) and (7) leads to

$$\varphi \approx \arctan\left(\pi \cdot 750 \cdot \frac{L \cdot P_1 \cdot I_q}{U_{emf}}\right). \quad (8)$$

Table III shows that the product of L and P_1 are constant approximately. However, with the increase of P_1, U_{emf} decreases and I_q increases, resulting in an increase of φ and low power factor.

C. Loss and Efficiency

The loss and the efficiency are shown in Fig. 7, considering the iron loss and the copper loss. The iron loss and the pole numbers are in positive correlation.

Equation (3) indicates that the torque current angular frequency is proportional to P_1. Thus, the increase of P_1 results in high iron loss. The copper loss is proportional to the square of the torque current, thus, the increase of the pole number will also result in high copper loss. Therefore, choosing a less pole number leads to higher efficiency.

IV. Suspension Performance Comparision

A. Magnitude Comparision

Fig. 8 shows the analysis results of the suspension force and the suspension current when the torque is set to a half of the rated value. The target of the suspension force is 155N with a suspension current less than 20A. The suspension force of 6-4 and 8-6 are small and below the target value within 20A. The suspension forces of all combinations show a good linear relation with the suspension currents except for the combination 4-2, of which the suspension force is saturated because of magnetic saturation.

There are 36 slots with two layers of suspension windings, thus, the per-pole-per-phase winding number N is calculated as

$$N = \frac{36 \times 2}{3 \cdot P_2} = \frac{24}{P_2}. \quad (9)$$

In the 4-2, combination with the biggest N=12 that is the highest. This can be seen in Fig. 3. Thus, the suspension magnetic field of 4-2 is tend to be saturated when high current is provided in suspension windings.

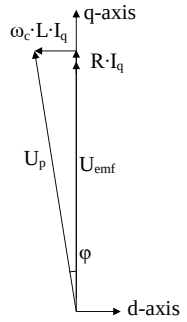

Figure 6. Phasor diagram.

TABLE III. Power Factor and Phase Inductance.

P_1	cosφ	L[10^{-5}H]	L·P_1[10^{-5}H]
2	0.86	7.5	15
4	0.86	3.1	12.4
6	0.81	2.4	14.4
8	0.71	1.8	14.4

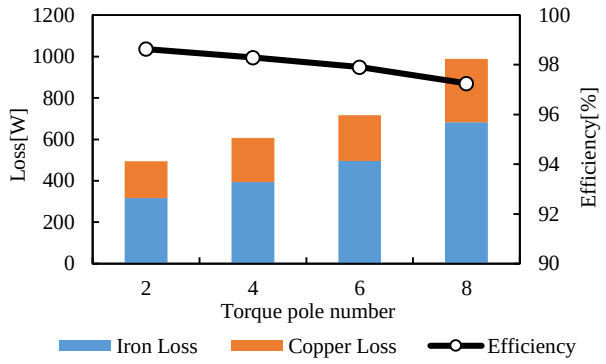

Figure 7. Power loss and efficiency.

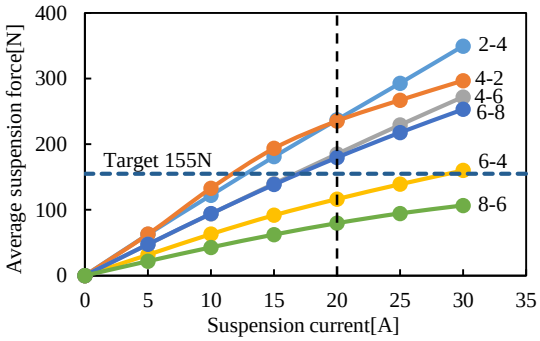

Figure 8. Suspension force.

B. Fluctuation Comparision

Fig. 9 shows the suspension force fluctuations under a half of the rated torque and suspension force of 155N. Combinations of 6-4 and 8-6 are excluded from the comparison because the suspension force did not reach the target.

The combination of 2-4, 4-2, 4-6 and 6-8 are compared. Only 2-4 has notable force fluctuation. The PM flux density of 2-4 in the airgap is close to a square wave rather than a sinusoidal wave, thus, force fluctuation is apparent. This may be eliminated by more careful winding design and skew, but this is a future project.

V. EDDY CURRENT COMPARISON

When the motor rotates, due to the relative speed between the rotor and the magnetic field, eddy current is generated in PMs and the shaft. In a low-speed motor, the relative speed is small, thus, the eddy current effect can be neglected. However, in a high speed motor, due to the large relative speed, a large eddy current may be generated and affect the suspension force. In Fig. 10, the eddy current density in the rotor of 4-2 is shown.

Table IV shows the comparison of eddy current when the torque current is zero and the suspension current is 10 A. It is found that the eddy current loss of 4-2 is the largest and the suspension force decreases by 10.3%. However, in other combinations, both eddy current loss and suspension force variation are very limited.

The relative speed between the rotor and the suspension magnetic field is the most important factor for the generation of eddy current. The rotation speed is 45000 r/min, which remains unchanged in all combinations. The torque magnetic field synchronizes with the rotor speed. However, due to the different pole numbers, the relative speed of the suspension magnetic field and the rotor is calculated as

$$\triangle n = \left| 45000 - \frac{45000 \cdot P_1}{P_2} \right| = \frac{90000}{P_2} \, r / \min . \qquad (10)$$

Fig. 11 shows the relationship between the relative speed △n and the eddy current loss. A positive correlation is roughly seen. Equation (10) indicates that the suspension pole number and the relative speed are in inversely proportional. Therefore, by choosing $P_2=P_1+2$, the relative speed can be reduced, which leads to smaller eddy current.

VI. CONCLUSION

In this paper, pole number comparison of a 45000 r/min and 35 kW BPM bearingless motor is presented. A proper combination of the torque and the suspension pole number is needed.

Table V shows the conclusion of comparisons. The performance of the cosφ, efficiency, suspension force and the PM eddy current, are compared. It is shown that a smaller torque pole number leads to high power factor and efficiency. The combinations of $P_2=P_1+2$ can generate large suspension force and less PM eddy current. 4-6 generates high suspension force with less force fluctuation. Therefore, 4-6 is shown to be the optimum pole number combination for the discussed BPM bearingless motor. However, 2-4 only has force fluctuation. If the force fluctuation can be reduced by further winding improvement, skew or PM arrangement, the efficiency, power factor and force are the best performance, thus, 2-4 also has a great possibility.

VII. ACKNOWLEDGMENT

This research is carried out with the support of JMAG academic. The authors would like to thank JMAG academic for JMAG software.

REFERENCES

[1] H. Mitterhofer, W. Gruber and W. Amrhein, "On the High Speed Capacity of Bearingless Drives," in *IEEE Transactions on Industrial Electronics*, vol. 61, no. 6, pp. 3119-3126, June 2014.

[2] T. Schneider and A. Binder, "Design and Evaluation of a 60 000 rpm Permanent Magnet Bearingless High Speed Motor," *2007 7th International Conference on Power Electronics and Drive Systems*, Bangkok, pp. 1-8, 2007.

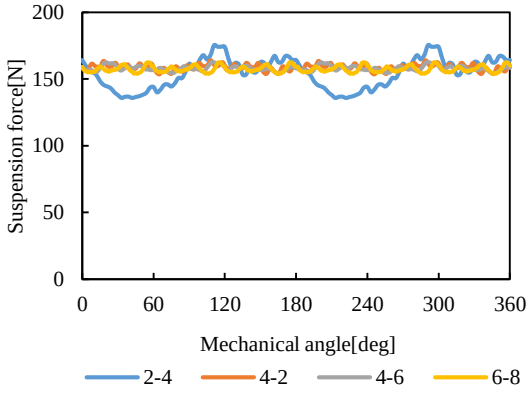

Figure 9. Suspension force fluctuation.

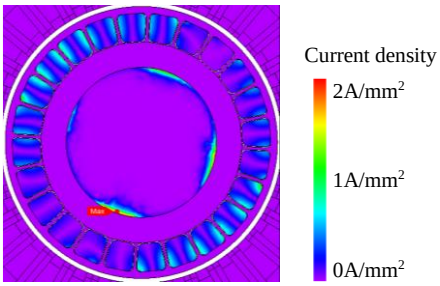

Figure 10. Eddy current in the rotor of 4-2.

TABLE IV. COMPARISON OF EDDY CURRENT.

P_1-P_2	Eddy Current Loss[W]	Suspension Force Variation[%]
2-4	0.9	0
4-2	4.9	-10.3
4-6	1.7	-0.4
6-4	1.3	-1.5
6-8	1.2	0
8-6	0.4	0

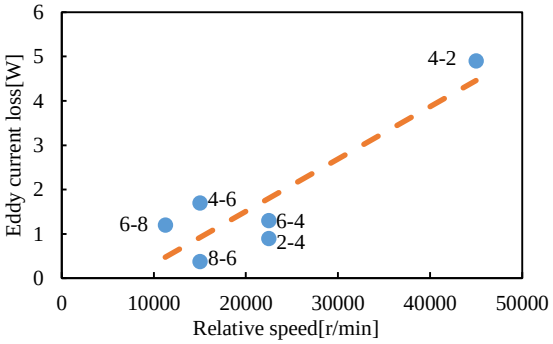

Figure 11. Relationship between relative speed and eddy current

TABLE V. CONCLUSION.

P_1-P_2	cosφ	Efficiency	Suspension force Amplitude	Suspension force Fluctuation	Eddy current
2-4	◎	◎	◎	△	○
4-2	◎	○	○	○	×
4-6	◎	○	○	○	○
6-4	△	○	×	-	○
6-8	△	○	○	○	○
8-6	×	△	×	-	○

◎:excellent ○:good △:acceptable ×:bad -:no result

[3] R. P. Jastrzebski, P. Jaatinen, O. Pyrhönen and A. Chiba, "Design of 6-slot inset PM bearingless motor for high-speed and higher than 100kW applications," *2017 IEEE International Electric Machines and Drives Conference (IEMDC)*, Miami, FL, pp. 1-6, 2017.

[4] P. Jaatinen, R. P. Jastrzebski, H. Sugimoto, O. Pyrhönen and A. Chiba, "Optimization of the rotor geometry of a high-speed interior permanent magnet bearingless motor with segmented magnets," *2015 18th International Conference on Electrical Machines and Systems (ICEMS)*, Pattaya, pp. 962-967, 2015.

[5] Y. Fu, M. Takemoto, S. Ogasawara and K. Orikawa, "Investigation of a high speed and high power density bearingless motor with neodymium bonded magnet," *2017 IEEE International Electric Machines and Drives Conference (IEMDC)*, Miami, FL, pp. 1-8, 2017.

[6] T. Schneider, J. Petersen and A. Binder, "Influence of pole pair combinations on high-speed bearingless permanent magnet motor performance," *2008 4th IET Conference on Power Electronics, Machines and Drives*, York, pp.707-711, 2008.

[7] Y. Okada, K. Dejima and T. Ohishi, "Radial position control of a PM synchronous type and induction type rotating motor," *Proceedings of 1994 IEEE Industry Applications Society Annual Meeting*, Denver, CO, pp. 234-239, 1994.